ELSEVIER

Available online at www.sciencedirect.com

SCIENCE DIRECT®

Computational Materials Science 33 (2005) 132–135

COMPUTATIONAL MATERIALS SCIENCE

www.elsevier.com/locate/commatsci

Application of X-ray standing wave (XSW) technique for studies of Zn incorporation in InP epilayers

A.A. Sirenko [a,*], A. Ougazzaden [b], A. Kazimirov [c]

[a] *New Jersey Institute of Technology, University Heights, Newark, NJ 07102-1982, USA*

[b] *Laboratoire Matériaux Optique, Photonique et Systèmes (MOPS), Université de Metz/Supelec, 57070 Metz, France*

[c] *Cornell High-Energy Synchrotron Source (CHESS), Cornell University, Ithaca, NY 14853, USA*

Abstract

We present a new approach to determine the site incorporation of p-type impurities in the doped layers of microelectronic device structures based on X-ray standing wave (XSW) technique. Activation behavior of Zn in InP epitaxial layers grown by metal organic vapor phase epitaxy (MOVPE) on InP(100) substrates has been studied. The XSW experiments were performed at the A2 beamline of the Cornell high-energy synchrotron source (CHESS). Angular dependences of the Zn–K fluorescence intensity excited by the XSW field inside the InP layer for symmetrical (400) reflection have been measured along with the Indium L-edge and phosphorus K-edge fluorescence and X-ray reflectivity. Analysis of the XSW data based on the dynamical diffraction theory in layered crystal structures allowed us to determine the fractions of both Zn atoms incorporated into crystal lattice and interstitial Zn. In our example, a 1 μm thick MOCVD-grown InP layer with the nominal concentration of Zn atoms of $(2.4 \pm 0.2) \times 10^{18}$ cm^{-3} has the fraction of the substitutional Zn of (65 ± 5)%. This result is in a good agreement with electrical activation of Zn measured with a combination of SIMS and CV profilometry. The accurate knowledge of the interstitial-to-substitutional ratio as a function of growth conditions is required to optimize electrical activation of Zn and to control its diffusion in the device structures.

© 2004 Elsevier B.V. All rights reserved.

1. Introduction

One of the common acceptor dopant in InP-based optoelectronic device structures grown by metalorganic vapor phase epitaxy (MOVPE) is Zn. Compared to other acceptors, such as Cd, Mg, and Be, which can also be used in InP–InGaAsP or InP–InGaAlAs material systems, Zn has superior solubility and lower ionization energy, the latter results in advantageously high degree of electrical activity of Zn at room temperature [1,2]. However, the main disadvantage of the Zn

* Corresponding author. Tel.: +1 973 596 5342; fax: +1 973 596 5794.

E-mail address: sirenko@njit.edu (A.A. Sirenko).

0927-0256/$ - see front matter © 2004 Elsevier B.V. All rights reserved.
doi:10.1016/j.commatsci.2004.12.028

acceptor is its nonintentional diffusion during the MOVPE growth that changes the post-growth Zn profile in InP layers [3] and, consequently, affects the device characteristics [4]. For example, uncontrolled diffusion of Zn can displace the desired position of the p–i–n junction and change the build-in electric field in the active region of the device that usually destroys the performance of the high-speed optoelectronic components.

To address this issue, extensive studies have been carrier out on Zn diffusion in InP and related materials, resulted in a common agreement that Zn diffusion during the growth can be generally described by substitutional–interstitial mechanism: interstitial zinc $Zn^{(i)+}$ diffuses until it is captured at vacancies of In-sublattice V_{In}^{-} to form substitutional zinc $Zn^{(s)-}$ [5]:

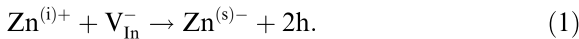

$$Zn^{(i)+} + V_{In}^{-} \rightarrow Zn^{(s)-} + 2h. \quad (1)$$

The p-type carrier concentration is determined mostly by the substitutional fraction of Zn that behaves as a shallow acceptor. In contrast, the interstitial Zn does not contribute to the p-type carrier concentration and is not electrically active in this sense. Thus, in the attempt to suppress zinc diffusion keeping the conductivity of the InP layer at maximum, great care should be taken to minimize the interstitial fraction of Zn.

The standard approach to control Zn incorporation and activation in InP-based structures grown by MOVPE is a combination of secondary ion mass spectroscopy (SIMS) and electrochemical capacity–voltage (CV) profiling. The total concentration of Zn ions N_{Zn} can be measured with SIMS using ion-implanted standards for calibration, while CV profiles provide the net electrically active carrier concentration, which is equal to the concentration of the substitutional Zn. Combining results of SIMS and CV profiling techniques, one can determine the Zn activation p/N_{Zn} as a function of the etched depth into the crystal:

$$p/N_{Zn} = N(Zn^{(s)})/(N(Zn^{(s)}) + N(Zn^{(i)})). \quad (2)$$

However, the absolute accuracy of SIMS and CV techniques is of the order of ±10% that results in a significant uncertainty in the impurity activation values. Moreover, the profiling approach is destructive by its nature and has low spatial resolution. In this paper we address this problem of precise control of the Zn acceptor behavior in InP layers by means of nondestructive X-ray standing waves (XSW) technique.

2. Experimental technique

For over two decades, the XSW technique was successfully applied to the studies of nearly perfect crystals and their surface structure. This technique is based on the interference field generated in and above the crystal due to superposition of incident and Bragg diffracted X-ray electromagnetic waves [6–8]. The periodicity of the standing wave is the same as that for the diffraction planes d_{hkl}. As the crystal is scanned through the Bragg peak, the standing wave field shifts inward by the half of its period ($d_{hkl}/2$) in the direction normal to diffraction planes. This movement modulates the interaction of the total electric field of the X-ray wave with atoms in the crystal lattice resulting in a pronounced angular dependence of the X-ray photoelectron absorption that can be observed by monitoring the fluorescence yields. The angular dependence of the fluorescence yield $Y(\theta)$ from atoms of a diffracting crystal can be written as

$$Y(\theta) = 1 + R(\theta) + 2f_H \cdot \cos(v(\theta) - 2\pi P_H)[R(\theta)]^{\frac{1}{2}}, \quad (3)$$

where $R(\theta)$ is the reflectivity, $v(\theta)$ is the phase of the diffracted plane wave, and P_H and f_H are the phase and modulus of the Hth Fourier component of the atomic distribution function projected onto the crystal unit cell. Thus, measuring the fluorescence yield from both doping atoms (Zn) and the host atoms (In and P), we can determine atomic position of impurity relative to the host unit cell, separating the interstitial and substitutional fractions of impurity.

3. Results and discussion

A micron-thick Zn-doped InP layer was grown on sulfur-doped 2-inch InP (1 0 0) substrate by liquid phase MOVPE in EMCORE reactor at the

growth temperature of 600 °C. The total atomic concentration of Zn measured with SIMS is $2.4 \times 10^{18}\,\mathrm{cm}^{-3}$ and p-type carrier concentration of $1.2 \times 10^{18}\,\mathrm{cm}^{-3}$ has been determined with electrochemical CV. Based on these measurements, we can determine the fraction of the substitutional Zn to be about (50 ± 10)%. The thickness of the Zn-doped layer was estimated to be 0.98 ± 0.05 μm based on a combination of SIMS and CV profiles, growth rate calibration, and SEM images.

XSW experiments were performed at the A2 wiggler beamline at CHESS. The X-ray beam size was about 1 mm. Principle components of our set-up are Si(1 1 1) double-crystal monochromator, the four-circle X-ray diffractometer, and XYZ sample positioning system. Typical angular resolution in our measurements was 11 arc seconds. We utilized X-ray radiation form the storage ring with the wavelength of 0.124 nm (energy of 10 KeV). Bragg diffraction was measured by scanning $\theta - 2\theta$ axes of the diffractometer. Fluorescence spectra have been measured with the energy-dispersive XFlash detector.

Fig. 1 shows fluorescence spectrum of our InP:Zn sample that is dominated by the strong indium-related $L_{\alpha 1,2}$, $L_{\beta 1,2}$ and $L_{\gamma 1}$ fluorescence lines between 3.28 and 3.92 KeV. The phosphorus $K_{\alpha 1,2}$ and $K_{\beta 1}$ fluorescence was measured between 2.01 and 2.14 KeV. The weak Zn-related $K_{\alpha 1,2}$ fluorescence signal was integrated between 8.62 and 8.64 KeV.

The experimental XSW data for the 0 0 4 reflection are shown in Fig. 2. Angular dependences of the fluorescence yield from In and P host atoms and Zn doping atoms are plotted together, along with the reflectivity curve. The curves of the In and P fluorescence yield look similar, as it should be for 0 0 4 reflection, where both In and P atoms belong to the same *diffraction* plane. Zn fluorescence repeats the main features of the host atom signal, as expected for the significant fraction of substitutional impurities. XSW data measured at other reflections (0 0 2 and 1 1 1) demonstrated that substitutional Zn (as expected for acceptor impurity) occupies In sites. Exact information about Zn locations in InP lattice was obtained based on analysis of our data using dynamical diffraction theory. Using the fit between the model and experimental data (shown in Fig. 3), the fractions of the interstitial and substitutional Zn have been measured to be 35% and 65%, respectively, with accuracy of ±5%. In this model, we assumed that the

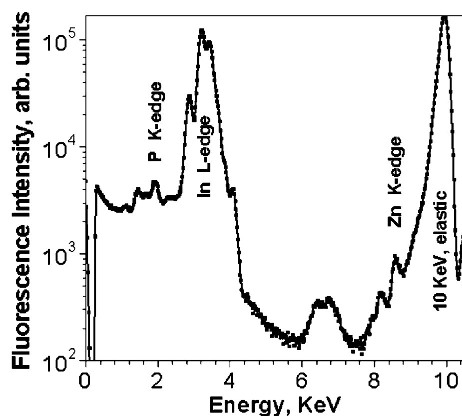

Fig. 1. Fluorescence spectrum of MOVPE-grown 1 μm-thick InP epilayers with the Zn concentration of $2.4 \times 10^{18}\,\mathrm{cm}^{-3}$. X-ray fluorescence spectrum is dominated by In-related band between 3.28 and 3.92 KeV and P-related fluorescence at 2 KeV. The weak acceptor Zn $K_{\alpha 1,2}$ fluorescence is at 8.6 KeV. The fluorescence excitation energy is 10 KeV.

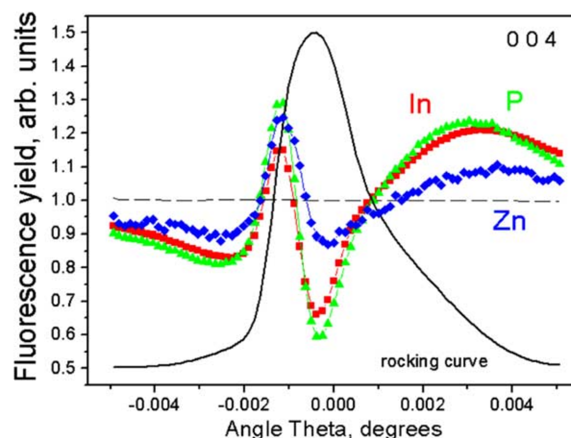

Fig. 2. Angular dependence of the relative variation of the fluorescence yield from In (squares), P (triangles), and Zn (diamonds) atoms along with the X-ray reflectivity curve (solid line) in the Zn-doped InP epilayer measured at the (0 0 4) reflection. Data are normalized for the fluorescence yield at the off-Bragg condition. The rocking curve is normalized to the maximum of reflection at the Bragg angle.

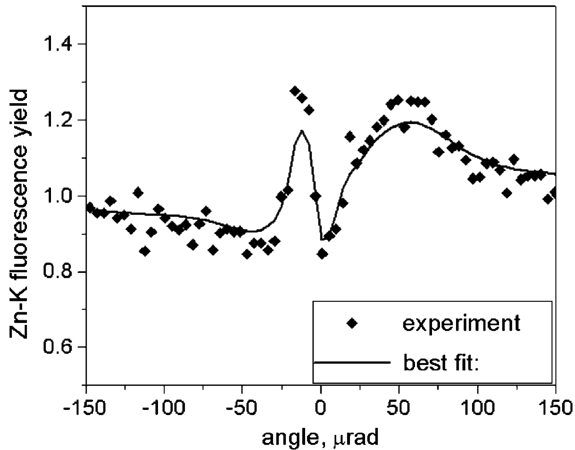

Fig. 3. The XSW results for the Zn fluorescence measured for (004) reflection and the best fit based on the dynamical diffraction theory in layered crystal structures. The fractions of the interstitial and substitutional Zn are determined from the best agreement between the fit and experimental data.

interstitial Zn is randomly distributed in the lattice, which is reasonable for the situation with many possible interstitial positions of Zn atoms. Assuming that the substitutional Zn is electrically active, while the interstitial Zn is not, we conclude that the XSW results for Zn activation are in a reasonable agreement with the aforementioned data for p/Zn ratio measured with SIMS and CV profilometry in the same sample: (50 ± 10)%. The future development of our experimental technique will include simultaneous analysis of XSW data taken at different reflections: (002), (111), (022), and (004). It should increase the accuracy of our measurements and will help to build up a more realistic 3D model for Zn incorporation in InP.

4. Conclusions

We demonstrated the experimental possibility to measure and analyze the impurity-related fluorescence signal using nondestructive XSW technique in epitaxial layers of InP. We believe that X-ray standing wave technique can be successfully applied to other III–V materials and impurities, for example to Cd, and Ru-doped InP layers and Mg-doped GaN structures. The next important step in the development of the XSWs for nondestructive impurity analysis in III–V semiconductor structures is to combine this technique with X-ray micro-beams to achieve impurity activation analysis with micron-size spatial resolution.

Acknowledgments

Authors would like to thank L. Ketelsen for support and encouragement of this work and S.N.G. Chu for useful discussions. The experiments at Cornell High-Energy Synchrotron Source (CHESS) have been supported by the National Science Foundation and the National Institutes of Health/National Institute of General Medical Sciences under award DMR 9713424.

References

[1] S.N.G. Chu, R.A. Logan, M. Geva, N.T. Ha, Concentration dependent Zn diffusion in InP during metalorganic vapor phase epitaxy, J. Appl. Phys. 78 (5) (1995) 3001–3007.
[2] R.A. Logan, S.N.G. Chu, M. Geva, N.T. Ha, C.D. Thurmond, Zn incorporation into InP grown by atmospheric pressure metalorganic vapor phase epitaxy, J. Appl. Phys. 79 (3) (1996) 1371–1377.
[3] M. Glade, J. Hergeth, D. Grutzmacher, k. Masseli, P. Balk, Diffusion of Zn acceptors during MOVPE of InP, J. Cryst. Growth 108 (1991) 449–454.
[4] H. Jung, P. Marschall, Zinc diffusion across the heterojunction in InP/InGaAsP heterostructures, JJAP 27 (1988) L2112–L2114.
[5] S.N.G. Chu, R.A. Logan, M. Geva, R.F. Karlicek, Substitutional, interstitial, and neutral zinc incorporation into InP grown by atmospheric pressure metalorganic vapor phase epitaxy, J. Appl. Phys. 80 (6) (1996) 3221–3227.
[6] V.G. Kohn, On the theory of X-ray diffraction and X-ray standing waves in the multilayered crystal systems, Phys. Stat. Sol. (a) 231 (2002) 132–148.
[7] S.K. Andersen, J.A. Golovchenko, G. Mair, New applications of X-ray standing-wave fields to solid state physics, Phys. Rev. Lett. 37 (1976) 1141–1145.
[8] A. Kazimirov, J. Zegenhagen, M. Cardona, Isotopic mass and lattice constant: X-ray standing wave measurements, Science 282 (1998) 930–932.